J|A|C|S
ARTICLES
Published on Web 06/05/2004

Proton-Coupled Electron Transfer of Flavodoxin Immobilized on Nanostructured Tin Dioxide Electrodes: Thermodynamics versus Kinetics Control of Protein Redox Function

Yeni Astuti,[†] Emmanuel Topoglidis,[†] Paul B. Briscoe,[‡] Andrea Fantuzzi,[‡] Gianfranco Gilardi,[‡] and James R. Durrant*[,†]

Contribution from the Departments of Chemistry and Biological Sciences, Imperial College London, South Kensington, London SW7 2AZ, U.K.

Received January 20, 2004; E-mail: j.durrant@imperial.ac.uk

Abstract: In this paper, we report a spectroelectrochemical investigation of proton-coupled electron transfer in flavodoxin *D. vulgaris* Hildenborough (Fld). Poly-L-lysine is used to promote the binding of Fld to the nanocrystalline, mesoporous SnO_2 electrodes. Two reversible redox couples of the immobilized Fld are observed electrochemically and are assigned by spectroelectrochemistry to the quinone/semiquinone and semiquinone/hydroquinone couples of the protein's flavin mononucleotide (FMN) redox cofactor. Comparison with control data for free FMN indicates no contamination of the Fld data by dissociated FMN. The quinone/semiquinone and semiquinone/hydroquinone midpoint potentials ($E_{q/sq}$ and $E_{sq/hq}$) at pH 7 were determined to be −340 and −585 mV vs Ag/AgCl, in good agreement with the literature. $E_{q/sq}$ exhibited a pH dependence of 51 mV/pH. The kinetics of these redox couples were studied using cyclic voltammetry, cyclic voltabsorptometry, and chronoabsorptometry. The semiquinone/quinone reoxidation is found to exhibit slow, potential-independent but pH-sensitive kinetics with a reoxidation rate constant varying from 1.56 s^{-1} at pH 10 to 0.0074 s^{-1} at pH 5. The slow kinetics are discussed in terms of a simple kinetics model and are assigned to the reoxidation process being rate limited by semiquinone deprotonation. It is proposed that this slow deprotonation step has the physiological benefit of preventing the undesirable loss of reducing equivalents which results from semiquinone oxidation to quinone.

Introduction

The chemical nature of the binding site of the redox cofactor in biological redox proteins is critical in determining the redox function of the cofactor. Differences in the protein environment can result in the same redox cofactor performing a broad range of functions, including electron or atom transfer, substrate activation and or conversion, and ligand binding.[1,2] The acid/base properties of the binding site are a key factor in influencing this functionality. Many biological redox reactions involve the uptake or release of protons from the cofactor and/or its protein environment. It is well established that such protonation/deprotonation events can have a strong influence on the thermodynamics of the reaction and result in a pH-dependent reaction free energy.[3] In addition to this widely established thermodynamic control of redox function, attention is increasingly focused on the importance of protonation/deprotonation events in influencing the kinetics of the overall redox reaction,[4−6] and thereby physiological function.

One of the most ubiquitous redox cofactors employed by nature is the isoalloxazine ring or "flavin", the prosthetic group of the large class of flavoproteins. This redox cofactor can undergo both one- and two-electron reduction, resulting in the formation of the singly reduced semiquinone and doubly reduced hydroquinone states. One or both of these reduction steps are typically directly coupled to protonation of the isoalloxazine ring. This range of redox properties allows flavoproteins to fulfill a diverse range of biochemical functions, including their functions in organic molecule hydroxylation in Class II cytochrome P450's and O_2 consumption in glucose oxidase.[2] One class of flavoproteins, flavodoxins (Fld), are small (15−20 kDa) electron-transferring proteins that have the flavin mononucleotide (FMN) as the redox cofactor noncovalently bound to a single polypeptide. Flavodoxins are widely distributed among various types of microorganisms where they can replace ferredoxins as electron mediators for a number of biological transformations.[2,7−14] The redox functions of Fld proteins are

[†] Department of Chemistry.
[‡] Department of Biological Sciences.

(1) Chapman, S. K.; Simon, D.; Munro, A. W. *Struct. Bonding* **1997**, *88*, 39−70.
(2) Muller, F. *Topics in Current Chemistry*; Springer, Berlin, 1981; Vol. 108, pp 71−108.
(3) Krishtalik, L. I. *Biochim. Biophys. Acta* **2003**, *1604*, 13−21.
(4) Brzezinski, P. *Biochemistry* **1996**, *35*, 5611−5615.
(5) Rappaport, F.; Lavergne, J. *Biochim. Biophys. Acta* **2001**, *1503*, 246−259.
(6) Hirst, J.; Duff, J. L. C.; Jameson, G. N. L.; Kemper, M. A.; Burgess, B. K.; Armstrong, F. A. *J. Am. Chem. Soc.* **1998**, *120*, 7085−7094.
(7) Dubourdieu, M.; le Gall, J.; Favaudon, V. *Biochim. Biophys. Acta* **1975**, *376*, 519−32.
(8) Simondsen, R. P.; Tollin, G. *Mol. Cell. Biochem.* **1980**, *33*, 13−24.
(9) Odom, J. M.; Peck, H. D., Jr. *Annu. Rev. Microbiol.* **1984**, *38*, 551−592.
(10) Thorneley, R. N. F.; Deistung, J. *Biochem. J.* **1988**, *253*, 587−595.
(11) Mayhew, S. G.; Tollin, G. *Chemistry and Biochemistry of Flavoenzymes III*; CRC Press: Florida, 1992; Vol. 3, pp 389−426.
(12) Ludwig, M. L.; Luschinsky, C. L. *Chemistry and Biochemistry of Flavoenzymes III*; CRC Press: Florida, 1992; Vol. 3, pp 427−467.
(13) Setif, P. *Biochim. Biophys. Acta* **2001**, *1507*, 161−179.

Scheme 1. Redox Chemistry of Flavodoxin and Its Physiological Functions

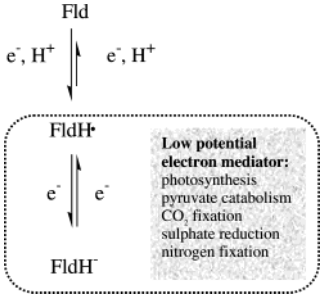

summarized in Scheme 1. The first reduction step is coupled to proton uptake, leading to the formation of the neutral semiquinone FldH•, resulting in a pH-dependent reduction potential.[7,15] In contrast, the second reduction step is not coupled to proton uptake at physiological pH's and results in the formation of the hydroquinone anion $FldH^-$.[2,12]

The thermodynamics of the Fld protein redox function are remarkably different from those of their protein-free cofactor FMN. The quinone/semiquinone and semiquinone/hydroquinone midpoint potentials ($E_{q/sq}$ and $E_{sq/hq}$, respectively) of Fld have been determined from solution redox titrations as $E_{q/sq} = -346$ and $E_{sq/hq} = -643$ mV vs Ag/AgCl (3.5 M KCL).[15] In contrast, the corresponding potentials for free FMN are $E_{q/sq} = -517$ and $E_{sq/hq} = -327$ mV,[16,17] inverted in order with respect to the protein-bound redox center. The inversion in the order of the two reduction potentials for Fld relative to free FMN represents a stabilization of semiquinone (FldH•) and destabilization of hydroquinone ($FldH^-$). This allows two consecutive one-electron reductions of Fld, between the Fld/FldH• at moderate negative potentials and subsequently between the FldH•/$FldH^-$ states at more negative potentials. In contrast, for free FMN, only the two-electron reduction of the quinone to the hydroquinone can be observed.[2,16−17] This inversion of redox potentials and the low midpoint potential of the FldH•/$FldH^-$ redox couple are both critical to the physiological function of flavodoxins. At typical cell potentials, the thermodynamically stable state of Fld is its quinone state. The physiological function of this protein is, however, generally thought be based on its low potential FldH•/$FldH^-$ redox couple,[2,8−14] with the thermodynamically favored oxidation of FldH• to Fld being physiologically undesirable.

The influence of the Fld binding site upon the redox chemistry of the FMN cofactor has been investigated by X-ray diffraction and NMR spectroscopy.[18−20] These studies have shown that formation of the Fld semiquinone is accompanied by protonation of the N(5) basic nitrogen of the flavin ring, consistent with the experimental observed dependence of the $E_{q/sq}$ midpoint potential upon solution pH. This protonation is stabilized by the formation, upon conformational changes, of a hydrogen bond between the carbonyl oxygen of Gly61 and N(5). The presence of this hydrogen bond has been suggested to be critical to the thermodynamic stabilization of FldH• as compared to the protein-free FMN semiquinone and therefore to the physiological function of Fld. The influence of this protonation upon the kinetics of the Fld redox chemistry has not received significant attention to date and is the primary objective of this paper. Previous studies have reported a pH dependency for oxidation of FldH• by O_2,[7,21,22] and for the reduction of cyt c by Fld,[23] although other studies have reported the reduction kinetics for the later donor/acceptor pair to be pH independent.[24] Such kinetics can be expected to be critical in avoiding the oxidation of the Fld semiquinone in vivo, this oxidation reaction being thermodynamically downhill at typical cell potentials but physiologically undesired.

Studies of flavodoxin redox function to date have largely been limited to solution redox titrations, stopped-flow spectrophotometry, and laser-flash photolysis.[7,15,21−24] Electrochemical studies of flavodoxins have been reported, including the use of a wide range of positively charged promoters such as aminoglycosides, poly-L-lysine (PLL), and sphermine to promote the binding of these negatively charged proteins on a range of different electrodes.[26−30] However, with the exception of the first publication in 1982,[26] such studies have been complicated by the release of the FMN cofactor from the protein, preventing observation of the Fld quinone/semiquinone redox couple. Heering and Hagen[30] proposed a complex model to describe the electrochemistry of flavodoxin *D. vulgaris* in which a combination of direct electron transfer, flavin-mediated electron transfer, and comproportionation play a role.

Armstrong and co-workers have shown that protein film voltammetry is a powerful approach to the study of kinetics of protein redox function.[6,27] In this paper, we employ a novel approach to protein film voltammetry, based upon the immobilization of Fld upon nanocrystalline, mesoporous SnO_2 electrodes. The high surface area and optical transparency of this electrode allow the use of optical spectroscopy to interrogate both the immobilization of protein upon such electrode and their subsequent electrochemistry under the application of electrical potentials.[31−34] We demonstrate that it is possible to achieve the stable immobilization of Fld upon these electrodes without significant denaturation or cofactor dissociation. Both the first and the second reduction potentials of the immobilized Fld are determined by potential step spectroelectrochemistry (spectro-

(14) Vervoort, J.; Heering, D.; Peelen, S.; Van Berkel, W. *Methods Enzymol.* **1994**, *243*, 188−203.
(15) Curley, G. P.; Voordouw, G. *FEMS Microbiol. Lett.* **1988**, *49*, 295−9.
(16) Anderson, R. F. *Biochim. Biophys. Acta* **1983**, *722*, 158−62.
(17) Mayhew, S. G. *Eur. J. Biochem.* **1999**, *265*, 698−702.
(18) Watenpaugh, K. D.; Sieker, L. C.; Jensen, L. H.; Legall, J.; Dubourdieu, M. *Proc. Natl. Acad. Sci. U.S.A.* **1972**, *69*, 3185−8.
(19) Watt, W.; Tulinsky, A.; Swenson, R. P.; Watenpaugh, K. D. *J. Mol. Biol.* **1991**, *218*, 195−208.
(20) Muller, F. *Chemistry and Biochemistry of Flavoenzymes III*; CRC Press: Florida, 1992; Vol. 3, pp 557−595.
(21) Mayhew, S. G.; Foust, G. P.; Massey, V. *J. Biol. Chem.* **1969**, *244*, 803−810.
(22) Edmonson, D. E.; Tollin, G. *Biochemistry* **1971**, *10*, 133−145.
(23) Pirola, M. C.; Monti, F.; Aliverti, A.; Zanetti, G. *Arch. Biochem. Biophys.* **1996**, *311*, 480−486.
(24) Franscesco, D. R.; Tollin, G.; Edmonson, D. E. *Biochemistry* **1987**, *26*, 5036−5042.
(25) Armstrong, F. A.; Wilson, G. S. *Electrochim. Acta* **2000**, *45*, 2623−2645.
(26) Van Dijk, C.; Van Leeuwen, J. W.; Veeger, C.; Schreurs, J. P. G. M.; Barendrecht, E. *Bioelectrochem. Bioenerg.* **1982**, *9*, 743−759.
(27) Armstrong, F. A.; Cox, P. A.; Hill, H. A. O.; Oliver, B. N.; Walton, N. J. *J. Am. Chem. Soc.* **1984**, *106*, 921−923.
(28) Bianco, P.; Haladjian, J.; Manjaoui, A.; Brusch, M. *Electrochim. Acta* **1988**, *33* (6), 745−752.
(29) Bagby, S.; Barker, P. D.; Hill, H. A. O.; Sanghera, G. S.; Dunbar, B.; Ashby, G. A.; Eady, R. R.; Thorneley, R. N. F. *Biochem. J.* **1991**, *277*, 313−319.
(30) Heering, H. A.; Hagen, W. R. *J. Electroanal. Chem.* **1996**, *404*, 249−260.
(31) Topoglidis, E.; Campbell, C. J.; Cass, A. E. G.; Durrant, J. R. *Langmuir* **2001**, *17*, 7899−7906.
(32) Topoglidis, E.; Astuti, Y.; Duriaux, F.; Gratzel, M.; Durrant, J. R. *Langmuir* **2003**, *19*, 6894−6900.
(33) Topoglidis, E.; Discher, B. M.; Moser, C. C.; Dutton, P. L.; Durrant, J. R. *ChemBioChem* **2003**, *4*, 1332−1339.
(34) Astuti, Y.; Topoglidis, E.; Gilardi, G.; Durrant, J. R. *Bioelectrochemistry* **2004**, *63*, 55−59.

potentiometry). The kinetics of the Fld redox function are addressed by cyclic voltammetry (CV) and its optical absorbance analogue, cyclic voltabsorptometry (CVA), and also by chronoabsorptometry (CA). CVA and CA have previously been introduced by Hawkridge and co-workers in the early 1980s to study diffusion-limited redox species.[35,36] By exploiting the optical transparency and high protein loading of our SnO_2 electrodes, we are able to extend such studies to investigate a layer of immobilized Fld. We note that the semiconducting nature of the SnO_2 electrode limits its exploitation to addressing the kinetics of fast electron-transfer reactions. However, we demonstrate that such electrodes are ideally suited to addressing relatively slow redox events and apply this approach here to a study of the kinetics of deprotonation associated with the oxidation of the Fld semiquinone to its quinone state.

Materials and Methods

Materials and Reagents. Flavodoxin *D. vulgaris* strain Hildenborough (Fld) was expressed and purified following the published procedure,[37] yielding a holoprotein with a purity index (RZ) of 4.3. FMN sodium salt and poly-L-lysine hydrobromide (PLL, molecular weight 1880) were obtained from Sigma-Aldrich and were used without further purification. All other chemicals were of reagent grade. Nanocrystalline, porous SnO_2 films were prepared on conducting glass substrates (TEC15 FTO, Hartford Glass, 15 Ω sq) as detailed previously.[32] The films comprised a porous network of SnO_2 nanocrystals, with surface area determined by BET analysis of 89 m^2 per g, corresponding to a film surface area of 300 cm^2 per 4 μm thick, 1 cm^2 macroscopic film area.[32]

Immobilization. A 25−30 μM solution of Fld or FMN was prepared in 5 mM potassium phosphate (KPi) buffer, pH 7. The PLL solution was prepared by dissolving 20 mg of transparent PLL powder in 4 mL of KPi buffer solution, pH 7. All aqueous solutions were prepared using distilled, deionized water of resistance 10 MΩ. Prior to immobilization, a 1 cm^2 area of SnO_2 electrode on FTO glass was heated at 450 °C for 20 min to remove all of the dirt and any adsorbed water. After being cooled, the SnO_2 electrode was then modified by immersion in PLL solution for 2 days. The electrodes were rinsed with KPi buffer and then immersed in Fld or FMN solution at 4 °C for up to 1 week, with the resultant protein adsorption being monitored by the film optical absorbance. Prior to all spectroscopic measurements, films were removed from the immobilization solution and rinsed in buffer solution to remove nonimmobilized protein. Contributions to the spectra from the scatter and absorption by the SnO_2 films alone were subtracted by the use of protein-free reference electrodes.

Electrochemistry. Potential control in electrochemical and spectroelectrochemical experiments was provided by Autolab PGSTAT 12 connected to a three-electrode spectroelectrochemical cell. The cell comprised a 3 mL single electrolyte compartment with quartz windows, employing a protein-free 0.014 M Kpi, pH 7, electrolyte, the SnO_2 film as the working electrode, a platinum mesh flag as the counter electrode, and an Ag/AgCl in 3.5 M KCl as the reference electrode. All potentials quoted are with reference to this electrode (203 mV vs NHE). The solution was thoroughly bubbled with argon for 20 min prior to experiments, with the anaerobic environment being maintained by keeping argon over the solution thereafter. For spectroelectrochemical studies, the cell was incorporated into the sample compartment of a Shimadzu UV-1601 spectrophotometer; optical absorbance spectra were recorded as a function of applied potential. For kinetic studies, cyclic voltammetry (measurement of the current as a function of potential) and cyclic voltabsorptometry (measurement of the optical absorbance as a function of potential) were conducted simultaneously, with the sample optical absorbance being monitored at a single probe wavelength. A more detailed discussion of the cyclic voltabsorptometry technique for the study of proteins immobilized on nanocrystalline SnO_2 films is given elsewhere.[34] Similarly, for chronoabsorptometry, the absorbance was monitored during the step potential. Differential cyclic voltabsorptometry data were obtained by differentiation of the CVA data with respect to the potential, followed by smoothing with a fast Fourier transform smoothing algorithm. A new sample was used for each pH. All experiments were carried out at ambient temperature.

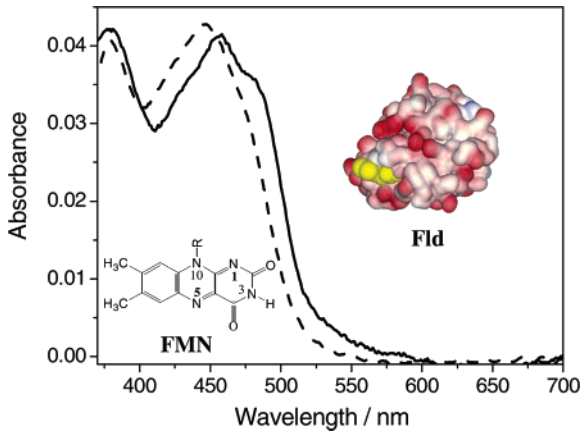

Figure 1. Absorption spectra of 4 μm Fld/SnO_2−PLL (−) and FMN/SnO_2−PLL (- - -) electrodes after subtraction of a blank SnO_2 electrode spectrum. Insets show the structure of FMN (R is ribitol phosphate) and the maps of the electrostatic potential representing those charges on the surface of Fld produced by DS Viewer. Positive potentials are shown in blue, negative potentials are shown in red, and neutral potentials are shown in white.

Results

Immobilization of Flavodoxin and FMN. Immersion of the PLL-treated SnO_2 electrodes in the Fld and FMN solutions resulted in a yellow coloration of the film, which saturated after ∼1−2 days immersion. Figure 1 shows the resulting film optical absorption spectra, in which the underlying SnO_2−PLL film absorbance and scatter have been subtracted by the use of protein-free control spectra. Omission of the PLL pretreatment of the SnO_2 resulted in negligible Fld immobilization upon the film. The spectrum of the protein-free FMN/SnO_2−PLL film exhibits absorption at 445 nm, characteristic of the solution spectrum of free FMN.[27] In contrast, the spectrum of the Fld/SnO_2−PLL electrode shows the characteristic 458 nm absorption maximum of protein-bound FMN, in good agreement with the solution spectrum of this protein,[8] and indicating that Fld immobilization does not result in significant protein denaturation or FMN dissociation.

The magnitude of the optical absorbance of the immobilized Fld and FMN can be employed to determine the loading on the film. Assuming extinction coefficients of 12 300 M^{-1} cm^{-1} at 445 nm for protein-free FMN and 10 700 M^{-1} cm^{-1} at 458 nm for Fld,[2,7] we obtain loading levels of 6 nmol/cm^2 for FMN and 4 nmol/cm^2 for Fld, consistent with our previous observation of immobilization of a range of protein on such metal oxide electrodes.[31−34] Assuming an area per Fld of 1000 Å,[2,19] the latter value corresponds to approximately monolayer coverage of Fld on the electrode surface. The immobilized Fld showed excellent stability, with no detectable denaturation over 2 weeks

(35) Bancorft, E. E.; Sidwell, J. S.; Blount, H. N. *Anal. Chem.* **1981**, *53*, 1390−1394.
(36) Cohen, D. J.; King, B. C.; Hawkridge, F. M. *J. Electroanal. Chem.* **1998**, *447*, 53−62.
(37) Krey, G. D.; Vanin, E. F.; Swenson, R. P. *J. Biol. Chem.* **1988**, *265*, 15436−43.

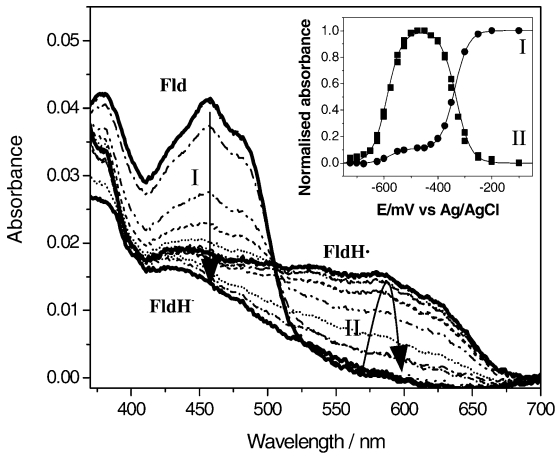

Figure 2. UV−vis spectral changes for the electrochemical reduction of the oxidized Fld/SnO_2−PLL under increasing negative potentials (0 to −725 mV vs Ag/AgCl). Insets show potentiometric titration data obtained by monitoring the change in absorbance at 460 nm (I) and 580 nm (II). All data were collected in 0.014 M KPi buffer solution, pH 7.

storage in protein solution, and no detectable desorption after half an hour bubbling with argon. In contrast, the free FMN was more weakly bound, achieving relatively low coverage of the electrode, and readily desorbing under, for example, bubbling with argon.

Spectroelectrochemistry. Following immobilization, the SnO_2 films were incorporated as the working electrodes in a spectroelectrochemical cell. Figure 2 shows typical spectroelectrochemical data obtained for a Fld/SnO_2−PLL film, demonstrating that the Fld can be cycled through its oxidized, semiquinone, and hydroquinone states by the application of electrical bias. The negative applied potential was increased in 25 or 50 mV steps, with the film being allowed to stabilize for 2 min before the optical absorbance spectrum was recorded. Complete stabilization of the absorbance spectrum was observed within this 2 min period for all biases, indicating all electroactive species reach thermodynamic equilibrium with the electrode within this time scale. Rather slower equilibration times were observed for the reverse oxidative potential steps, as we discuss in detail below. The application of potentials up to −450 mV vs Ag/AgCl results in the appearance of a broad absorption band between 400 and 700 nm, characteristic of the formation of the neutral semiquinone FldH·, which is blue in color.[7,8] Upon the application of more negative potentials, these broad absorption bands disappear, leaving a weak band at around 365 nm and a shoulder at 420 nm, characteristic of the formation of the hydroquinone anion state $FldH^-$.[7,8,12]

The inset to Figure 2 shows the optical absorbance at 580 nm versus applied potential, showing the growth of the semiquinone absorption, which is maximal at −450 mV, and the subsequent decay of this absorption at more negative potentials due to reduction of the semiquinone to the hydroquinone. Equally, these processes can also be seen as a two-slope graph when the absorbance at 460 nm was plotted. These potentiometric titration data were fitted (solid lines in inset to Figure 2) to the Nernst equation for two consecutive electron-transfer steps, yielding midpoint potentials for the first and second reduction steps of $E_{q/sq} = -340 \pm 0.93$ and $E_{sq/hq} = -585 \pm 0.91$ mV, respectively. For both steps, $n = 0.98 \pm 0.01$, consistent with both redox couples corresponding to single electron reductions/oxidations. The $E_{q/sq}$ value is in good

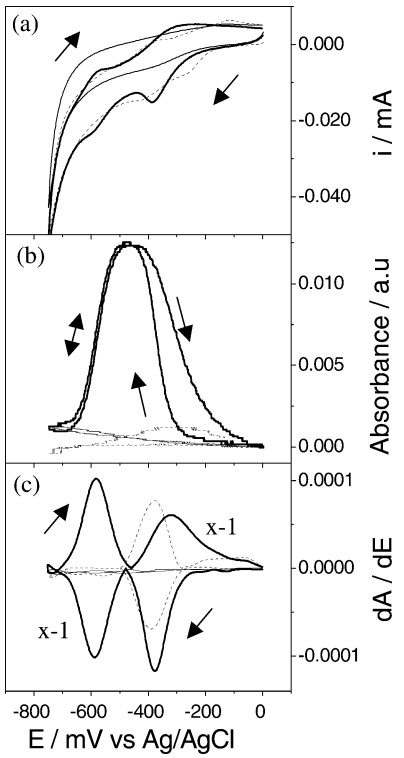

Figure 3. CVs (a), CVAs (b), and DCVAs (c) of Fld/SnO_2−PLL (bold line) and FMN/SnO_2−PLL (- - -) in comparison to a blank SnO_2−PLL electrode (fine line). Arrows show the scan directions. CVA data shown using a probe wavelength at 580 nm. DCVA data shown using probe wavelength at 580 nm (Fld/SnO_2−PLL and protein-free SnO_2 film) and 445 nm (FMN/SnO_2−PLL). To make the DCVA data readily comparable to CV, the second reduction and the first oxidation in the DCVA data were multiplied by −1. All experiments were measured at scan rates of 5 mV/s in a protein-free 0.014 M KPi buffer solution, pH 7.

agreement with that of −346 mV determined for Fld in solution by titration with dithionite.[15] The $E_{sq/hq}$ value exhibits a small positive shift as compared to potentials of −643 mV determined for Fld in solution [15] and of −613 mV at glassy carbon electrode.[30]

Control spectroelectrochemical data (not shown) for the protein-free FMN/SnO_2−PLL films showed no significant absorbance increase at any wavelength, but only an absorbance decrease leading to a weak residual absorbance characteristic of the hydroquinone. Fitting the change in absorbance at 445 nm to the Nernst equation gave the midpoint potential of −389 ± 4 mV with $n = 1.56 \pm 0.1$. This is in agreement with previous studies that electrochemical reduction of FMN leads directly to the two-electrons-reduced hydroquinone without the formation of a stable semiquinone intermediate.

Cyclic Voltammetry and Voltabsorptometry. The dynamics of redox function for the Fld/SnO_2−PLL and FMN/SnO_2−PLL films were monitored by cyclic voltammetry and voltabsorptometry. Typical data are shown in Figure 3. Figure 3a shows cyclic voltammograms (CVs) of Fld/SnO_2−PLL and FMN/SnO_2−PLL in addition to control data for a blank SnO_2−PLL electrode, all scanned at 5 mV/s. The background current observed for the blank SnO_2−PLL is assigned, as previously,[32] to charging/discharging of nanocrystalline electrode. In addition to this background current, CVs of the films with immobilized Fld and FMN show well-defined reduction and oxidation peaks. Two reversible redox couples can be observed for the CV of Fld/SnO_2−PLL, with midpoint potentials at −342 and −585

mV. These midpoint potentials are in good agreement with those observed in the spectroelectrochemical redox titration (Figure 2). For the FMN/SnO_2−PLL electrode, only a broad peak can be observed with a midpoint potential at −390 mV, in agreement with the spectroelectrochemical data for free FMN, with a smaller peak observed at more positive potentials, tentatively assigned to a different orientation of FMN binding. Similar broad peaks have been reported for CVs of FMN at different electrodes and attributed to the variation in FMN orientation to the electrode.[28,39] This FMN couple is not apparent in the CV of the Fld/SnO_2−PLL electrode, consistent with absence of protein-free FMN in this film as indicated by the optical absorbance spectra. These observations are in marked contrast to previous electrochemical studies of flavodoxins,[25−30] where the presence of free FMN has prevented unambiguous observation of the quinone/semiquinone couple of Fld.

The corresponding cyclic voltabsorptomograms (CVAs) are shown in Figure 3b, employing a detection wavelength of 580 nm to follow directly the formation of the Fld semiquinone (absorption maximum at 580 nm) and its subsequent reduction to the hydroquinone. For the Fld/SnO_2−PLL electrode, the formation of the semiquinone FldH· is clearly observed as a maximum in the absorbance during both the forward and the reverse scans. In contrast, the CVAs for both the blank and the FMN/SnO_2−PLL electrodes give negligible absorbance at this wavelength.

Direct comparison of the CV and CVA data can be most easily made by consideration of the derivative of the CVA signal, corresponding to the change in population of redox species with time, and proportional to the magnitude of the electrochemical current. First derivatives of CVAs are therefore expected to be morphologically identical to the "ideal" CV response for electrochemical processes. Such derivatives of the CVA data (DCVAs) are shown in Figure 3c. DCVAs are shown for the Fld- and FMN-coated films at 580 nm, and for the FMN-coated film probed at 445 nm, with the latter wavelength being selected to monitor the loss of quinone absorption due to its two-electron reduction to its hydroquinone state. It is apparent that the DCVA traces are indeed of similar structure to the corresponding CVs, with reduction and oxidation peaks being observed at similar potentials in all cases. However, because the optical signals are only sensitive to the redox couple contributing to the absorbance at the wavelength selected and can therefore be selected to be specific to the redox couple of interest, the DCVA traces are, in contrast to the CV data, essentially background free. As a consequence, it is apparent that the oxidation and reduction peaks for both the Fld and the FMN films are much better defined in the DCVA traces than in the corresponding CVs.

The midpoint potentials determined from these DCVA yield values for Fld of $E_{q/sq} = -342$ and $E_{sq/hq} = -587$, and for FMN $E_{q/hq} = -386$ mV, in agreement with the CV data. With the exception of the semiquinone to quinone oxidation peak, all of the redox peaks of the Fld/SnO_2−PLL film exhibit full widths at half-maximum (fwhm) of 100 mV, in reasonable agreement with theoretical expectations for one reversible electron reaction.

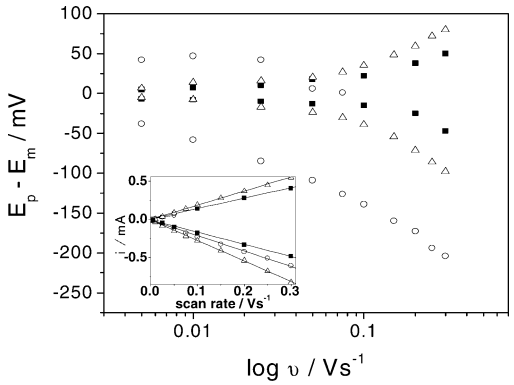

Figure 4. Plots of anodic and cathodic peak separations against the logarithm of the scan rate for FMN/SnO_2−PLL (■), and the first (○) and second (△) electron transfers of Fld/SnO_2−PLL electrodes. The inset shows plots of the cathodic and anodic peak currents versus scan rate.

For FMN, a larger peak fwhm of 111 mV is observed, indicative of less ideal behavior.

The kinetics of electron transfer were investigated by adjusting the scan rates. The CV peak separations were then plotted versus the scan rate, as shown in Figure 4. Ideal "trumpet" behavior[6,25] is observed for the FMN and FldH·/FldH$^-$ redox couples, indicative of fast, reversible electrochemistry. For the Fld/FldH· couple, nonideal behavior is observed, with the oxidation peak shifting to less positive potentials, broadening, and becoming less defined as the scan rate was increased. The origin of this behavior will be discussed below.

It is apparent from Figure 4 that the kinetics of the redox reaction are in the order fastest to slowest FMN/FMNH$^-$ > FldH·/FldH$^-$ > Fld/FldH·. Employing the Laviron approach,[40] electron-transfer rate constants for these three redox couples were determined to be 3.5, 2.5, and 0.6 s^{-1}. In all cases, the charge-transfer coefficient α was determined to be ∼0.50. For the Fld/FldH· couple, the absence of a well-behaved oxidation peak clearly limits the validity of this analysis, and the rate constant of 0.6 s^{-1} should only be taken as an approximate value of the rate constant, only applicable to the reductive reaction.

pH Dependence. Figures 5−8 address the influence of pH on Fld/SnO_2−PLL redox chemistry. Potentiometric titrations such as that shown in Figure 2, inset, were carried out as a function of pH. The resulting Fld/FldH· and FldH·/FldH$^-$ midpoint potentials are plotted as a function of pH in Figure 5 (open symbols). Also plotted in this figure are the midpoint potentials obtained from potential sweep experiments (CV and CVA) at scan rates of 5 mV/s (solid symbols). The potentiometric titration data were fitted to the equation for redox-linked protonation,[41] in which E_{alk} is the limiting value of the reduction potential at high pH where no proton is transferred.

$$E_{(pH)} = E_{alk} + \frac{RT}{nF}\ln\left(1 + \frac{[H^+]}{K_{red}}\right) \qquad (1)$$

In the pH range 4−10, the value of the Fld/FldH· midpoint potential ($E_{q/sq}$) shows a linear dependency upon pH, with a gradient of −51 mV/pH and pK of ≥10, as expected with this reaction being associated with a protonation/deprotonation reaction. In contrast, the FldH·/FldH$^-$ midpoint potential ($E_{sq/hq}$)

(38) Yalloway, G. N.; Mayhew, S. G.; Malthouse, J. P. G.; Gallagher, M. E.; Curley, G. P. *Biochemistry* **1999**, *38*, 3753−3762.
(39) Shinohara, H.; Graetzel, M.; Vlachopoulos, N.; Aizawa, M. *Bioelectrochem. Bioenerg.* **1991**, *26*, 307−320.
(40) Laviron, E. *J. Electroanal. Chem.* **1979**, *101*, 19−28.
(41) Clark, W. M. *Oxidation−Reduction Potentials of Organic Systems*; Williams and Wilkins: Baltimore, MD, 1960.

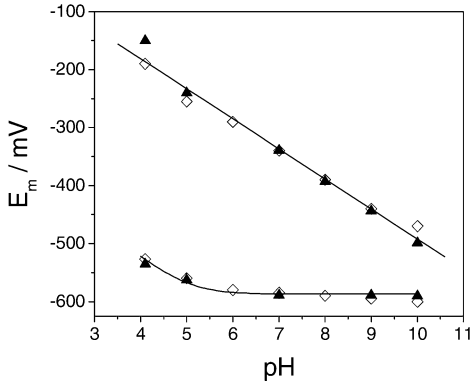

Figure 5. Midpoint potential for the Fld/FldH· and FldH·/FldH$^-$ couple of Fld/SnO_2−PLL as a function of potential determined by CVs (▲) and potentiometric titration (◇). The solid lines are the fitting of potentiometric titration data to the equation for redox-linked protonation, eq 1.

shows a weak pH dependence with a pK ∼5, consistent with this reaction not being significantly associated with proton exchange.

The pH dependence of the CV, CVA, and DCVA traces for an Fld/SnO_2−PLL film are shown in Figure 6. It is apparent from both the CV and the DCVA data that the second oxidation peak, corresponding to FldH· oxidation to Fld, is strongly pH dependent, shifting to more positive potentials, broadening, and reducing in amplitude as the pH is reduced. This observation can be most easily assigned to a retardation of the kinetics of the reaction under acidic pH. This retardation is most readily apparent in the CVA data, which clearly show a retardation of the decay of the FldH· absorbance at 580 nm at acidic pH. Confirmation of this assignment can be unambiguously made from the scan rate dependence of the CVA data. The half time for the decay of the semiquinone absorbance in the oxidative sweep of the CVA data was found to be independent of scan rate, demonstrating that the retardation apparent in Figure 6 derives from slow reoxidation kinetics, and not from thermodynamic inhomogeneity.

The kinetics of the redox chemistry were further investigated by chronoabsorptometry, monitoring the optical absorbance as the potential stepped between the potential where the major species of the immobilized Fld is oxidized (0 mV), semiquinone (−500 mV at pH 10, −475 mV at pH 9 and 8, −460 mV at pH 7, and −450 mV at pH 5), and hydroquinone (−750 mV). Data are shown for two pH's, pH 5 and 10 (Figure 7). At pH 10, the optical signal exhibited a rapid response (<1 s) for all redox transitions. However, at pH 5, the final step from −500 to 0 mV, corresponding to the FldH· oxidation to Fld, exhibits a much slower response, consistent with the CVA reported above. This slow response was found to be monoexponential, with a first-order rate constant of 0.0074 s^{-1} at pH 5. This rate constant was found to be independent of the magnitude of the potential step, with steps from −500 mV to potentials ranging from −150 to 300 mV all yielding indistinguishable rate constants (see inset of Figure 7), indicating the reoxidation reaction is not rate limited by an electron transfer to the electrode. The resulting reaction rate constant $k_{sq/q}$ is plotted as a function of pH in Figure 8. It is apparent that the rate constant is pH dependent, showing a linear dependence of log $k_{sq/q}$ versus pH. Strikingly, this behavior is consistent with the solution studies of pH dependency of FldH· oxidation by O_2 reported by Duberdieu et al. in 1974.[7] However, we note the difference in the slope of both data, which is 0.5 and 0.9 per pH unit for our electrode system and Duberdieu's solution studies, respectively.

Discussion

Immobilization of Flavodoxin and FMN. We have demonstrated the successful immobilization of the flavodoxin, Fld, on nanocrystalline SnO_2 electrodes with a protein loading of 4 nmol/cm^2, corresponding to approximately monolayer coverage of the electrode surface. We have found that pretreatment of the SnO_2 film with poly-L-lysine is essential to achieve Fld immobilization. This pretreatment is most probably necessary due to unfavorable electrostatic interactions between the Fld and the untreated SnO_2 surface. At pH 7, both the SnO_2 electrode and the Fld are expected to be negatively charged (SnO_2 point of zero charge of ∼6, Fld isoelectric point of 3.6), resulting in electrostatic repulsion between them. PLL was then chosen as a binding promoter because this polycation has been shown previously to enhance the adsorption of several negatively charged proteins on Hg,[26] carbon-based,[30] and TiO_2 electrodes.[32,42] For FMN binding, electrostatic interactions between the PLL and the FMN phosphate group can again be expected to favor immobilization. For Fld, the presence of a ring of negative surface charge around the FMN binding pocket[45] can be expected to favor immobilization of the protein orientated in such a way as to enhance electron transfer between the FMN cofactor and the electrode surface, consistent with our observation of reversible electrochemistry.

Assignment of the Electrochemical Signal. Previous studies of Fld electrochemistry have all been complicated by the presence of protein-free FMN, preventing observation of the Fld/FldH· redox couple. In contrast, we have demonstrated here that Fld may be immobilized upon the SnO_2−PLL films without the presence or appearance of any significant amounts of protein-free FMN. Optical absorbance spectra of Fld/SnO_2−PLL electrodes before, during, and after electrochemical studies all indicated the absence of significant free FMN absorbance and indeed yield optical absorbance spectra in excellent agreement with solution spectra of Fld. Similarly, spectroelectrochemical studies of the optical absorbance changes associated with each reduction and oxidation event observed in the cyclic voltammetry allowed unambiguous assignment of each peak to a specific redox reaction. Comparison of CV and DCVA traces between Fld/SnO_2−PLL and control FMN SnO_2−PLL electrodes showed negligible presence of free FMN in the former electrodes. Finally, spectroelectrochemical studies of the optical absorbance changes associated with each reduction and oxidation event observed in the cyclic voltammetry of Fld/SnO_2−PLL allowed the assignment of the first reduction couple to the Fld/FldH· redox couple.

The absence of FMN dissociation upon immobilization to the electrode surface is in striking contrast to previous electrochemical studies of Fld. This excellent stability is, however, in agreement with solution studies which have shown a tight binding of FMN to apoprotein with a dissociation constant (K_d) as small as 0.24 nM.[15,43,44] It is, moreover, consistent with our

(42) Rodriguez, R.; Blesa, M. A.; Regazzoni, A. E. *J. Colloid Interface Sci.* **1996**, *177*, 122−131.
(43) Löhr, F.; Mayhew, S. G.; Rüterjans, H. *J. Am. Chem. Soc.* **2000**, *122*, 9289−9295.
(44) Mayhew, S. G.; O'Connell, D. P.; O'Farrell, P. A.; Yalloway, G. N.; Geoghegan, S. M. *Biochem. Soc. Trans.* **1996**, *24*, 122−127.
(45) Zhou, Z.; Swenson, R. P. *Biochemistry* **1995**, *34*, 3183−3192.

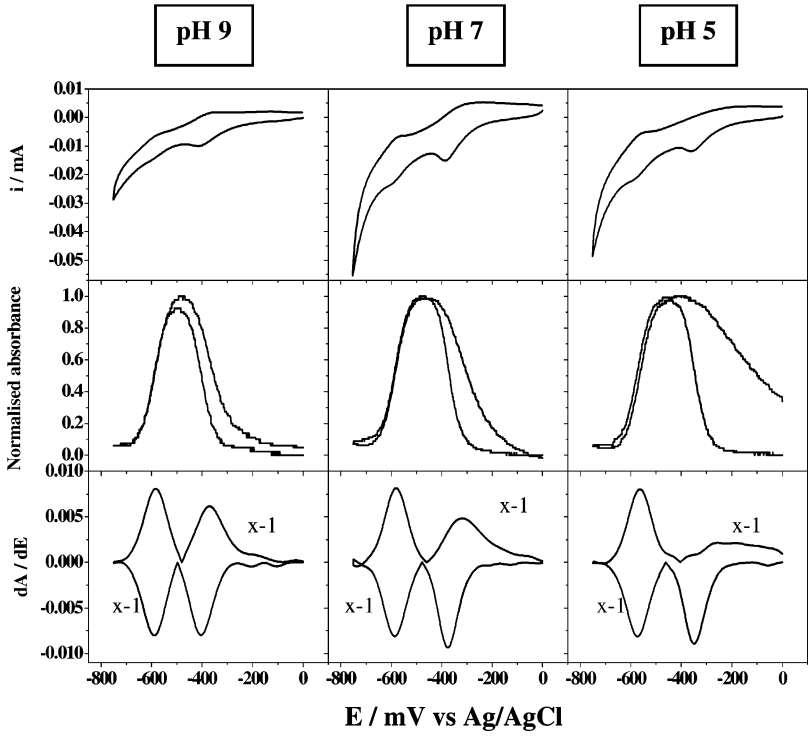

Figure 6. CVs, CVAs, and DCVAs of Fld/SnO_2−PLL. All experiments were measured at 5 mV/s in 0.014 M KPi buffer solution, pH 5, 7, 9. CVA and DCVA data employed a probe wavelength of 580 nm. Other details are as in Figure 3.

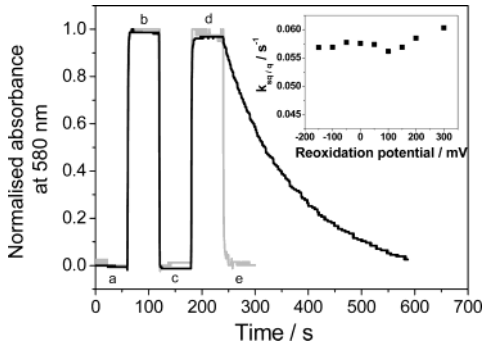

Figure 7. Typical chronoabsorptometry signal at pH 5 (black −) and pH 10 (gray −) showing the cycle of Fld redox states upon application of step potentials between 0 mV (a,e), −500 mV (pH 10, b,d), and −450 mV (pH 5, b,d) and −750 mV (c). The inset shows the dependence of the FldH·/Fld reoxidation rate constant obtained from such data at pH 7 as a function of the final potential of the electrode.

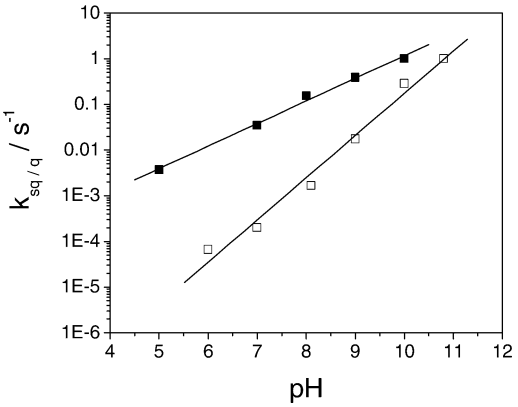

Figure 8. Plots of log $k_{sq/q}$ versus pH for reoxidation of FldH· by SnO_2−PLL electrodes (■), obtained from chronoabsorptometry data such as those shown in Figure 7. Also shown are the data taken from ref 10 for FldH· reoxidation by O_2 in solution (□).

previous observations that a wide range of proteins may be stably immobilized upon nanocrystalline metal oxide electrodes without significant denaturation or loss of protein function.[31−34] The excellent protein stability on these electrodes may be associated with the hydrophilic nature of the metal oxide surface. It may also result from conformational restraints resulting from retention of the protein within the small (∼10 nm diameter) pores of the film preventing protein denaturation. We further note that the expected binding orientation of the Fld on the electrode surface, with the FMN cofactor "sandwiched" between the electrode surface and the protein, can also be expected to impede FMN dissociation, stabilizing the binding of native Fld on the SnO_2−PLL electrodes.

We observe a positive shift in the FldH·/$FldH^-$ midpoint potential relative to those values obtained in solution studies, indicating energetically more favorable reduction. This shift is not observed for the Fld/FldH· couple, but is observed for the protein-free FMN/$FMNH^-$ couple. Recent reports by Swenson and colleagues[45,46] showed that neutralization of six acidic residues clustered around the binding site within 13 Å of the N(1) of FMN in Fld by site-directed mutation caused a positive shift in $E_{sq/hq}$ of 93 mV (about 15 mV per substitution), but a shift of only 14 mV for $E_{q/sq}$. This additive shift in $E_{sq/hq}$ upon neutralization of acidic residues was attributed to a general electrostatic effect,[45] supporting the idea that the hydroquinone is anionic. A similar electrostatic effect may account for the shift in the $E_{sq/hq}$ on our PLL-coated SnO_2 electrodes due to the presence of positively charged PLL at the protein/electrode interface. Both hydroquinone in Fld and FMN are likely to be anionic, thus being more susceptible to electrostatic perturbation by PLL than the neutral FldH·.

(46) Zhou, Z.; Swenson, R. P. *Biochemistry* **1996**, *35*, 15980−15988.

Scheme 2. Mechanism of Proton-Coupled Electron Transfer in Fld

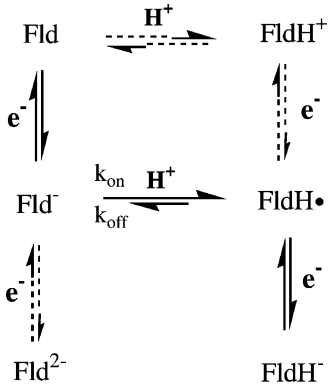

Electron-Transfer Dynamics. The cyclic voltammetry and voltabsorptometry data both indicate reversible electron transfer between the immobilized Fld and the electrode surface at slow scan speeds. This reversible electrochemistry is achieved without the use of any redox mediator and can therefore be assigned to direct electron transfer between the electrode surface and the redox species. FMN shows the fastest electron-transfer rate constant, consistent with its expected closer proximity to the metal oxide surface. For Fld, semiquinone/hydroquinone electron transfer is faster than the quinone/semiquinone couple, most probably attributed, as we discuss below, to the latter couple being coupled to proton transfer.

We note that the electron-transfer rate constants are relatively slow (0.6−3.5 s^{-1}) as compared to those more typically reported for small redox proteins immobilized upon metal or glassy carbon electrodes but typical of those we have reported previously for a range of redox proteins immobilized on nanocrystalline metal oxide electrodes.[30−34] These dynamics were found to be independent of electrode thickness, suggesting that they are not rate limited by charge transport through the metal oxide film (at least up to scan rates of 1 V/s) over the potential window employed in this study. More probably, the relatively slow interfacial electron dynamics can be attributed to the relatively sparse metal oxide density of electronic states as compared to metallic electrodes.

Proton-Coupled Electron Transfer. The scan rate dependence of the CV traces, as shown in Figure 4, suggests that the Fld semiquinone reoxidation step is not rate limited by the interfacial electron transfer, but rather by an alternative process. The studies as a function of pH presented in Figures 5−8 demonstrate that this rate-limiting process is associated with deprotonation of the semiquinone. The $E_{q/sq}$ shows a strong pH dependence, in contrast to the semiquinone/hydroquinone couple, which is essentially independent of pH. Most strikingly, the kinetics of the semiquinone oxidation, apparent in the CV, DCVA, and, most obviously, the CVA and CA data, show a marked retardation at acidic pH. The pH dependence of the $E_{q/sq}$ is in good agreement with previous studies. However, the dependence of the oxidation kinetics upon pH has only, to our knowledge, received limited attention to date.[7,21−24]

The kinetics of Fld redox function can be most readily considered in terms of a simple kinetic model, as illustrated in Scheme 2. Such simple models have been widely used previously in analysis of proton-coupled electron-transfer dynamics.[5,6] In this scheme, the vertical arrows correspond to electron-transfer reactions, and the horizontal arrows correspond to proton uptake/release. Double protonation of the hydroquinone is neglected, in agreement with previous studies.[7,12] Variation of the electrode potential results in variation of the free energy of electrode electrons, and therefore the free energies of reaction involving electron exchange with the electrode (the vertical arrows). Variation of the electrolyte pH results in variation in the free energy of the protons in the electrolyte, and therefore the free energies of reactions involving proton exchange with the electrolyte (the horizontal arrows).

According to the kinetic model shown in Scheme 2, reduction of the quinone Fld to the protonated semiquinone FldH· may in principle proceed via either of two intermediates: $FldH^+$ or Fld^-. Our experimental observations are not consistent with the reaction mechanism proceeding via the $FldH^+$ intermediate, which would result in slower and pH-dependent Fld reduction kinetics, rather than the slower and pH-dependent FldH· oxidation kinetics experimentally observed. This conclusion is in agreement with the low pK value of <1 reported previously for protonation of Fld at N(5),[2] indicating that formation of $FldH^+$ is highly unfavorable (ΔG > 34 kJ/mol at pH 7) except at very acidic pH's.

Our experimental data are most easily interpreted in terms of both the oxidation and the reduction reactions proceeding via the Fld^- intermediate. The pK for protonation of the semiquinone has been reported as >11,[2,7−15] indicating that, over the pH range of study, this equilibrium favors the protonated semiquinone FldH·. The reaction free energy for this equilibrium ΔG can be expected to be pH dependent, varying from −11 kJ/mol at pH 9 to −34 kJ/mol at pH 5. For this reason, the deprotonation step k_{off} will be slower than the protonation step k_{on}, consistent with deprotonation of the FldH· semiquinone rate limiting the semiquinone oxidation. The scan rate and oxidation potential (inset Figure 7) independency of the half time of semiquinone oxidation support this conclusion. Moreover, the pH dependency of FldH· oxidation observed in our electrode system is consistent with the data reported by Duberdieu et al., following FldH· oxidation by O_2.[7] The pH dependence of this oxidation can be readily understood in terms of an increase in the activation energy E_a for the deprotonation step k_{off} in Scheme 2, consistent with the larger positive ΔG for this reaction at acidic pH's, resulting in a retardation of k_{off} . The difference in the activation energy for both systems may account for the difference in the slope of Figure 8.

In addition to the retardation of the semiquinone reoxidation, the hydroquinone reoxidation is marginally retarded relative to the reduction dynamics, particularly at acidic pH (data not shown). This may be indicative of partial double protonation of the hydroquinone to form $FldH_2$, consistent with the pK of 5−6 reported for this protonation.[2,12,30] Again, the deprotonation process could rate limit the reoxidation step.

Physiological Importance. The studies we present here indicate that the proton coupling is important not only for thermodynamic but also kinetic control of Fld redox function. Protonation of the cofactor may partially account for the separation of the $E_{q/sq}$ and $E_{sq/hq}$ up to 300 mV,[2,8] allowing the two stepwise electron transfers to be occurred. The other contribution may come from the destabilization of the $FldH^-$ by accumulative changes in the dielectric local environment of the binding site.[45,46] This thermodynamic regulation is important

in allowing Fld to carry out its biological function as a one-electron-transferring protein that operates at low potentials, shuttling between the $FldH^{\bullet}$ and $FldH^{-}$ redox states.[2,7−15,47] In addition to this thermodynamic control, the experiments we report here indicate that the rate of the $FldH^{\bullet}$ oxidation is kinetically slow due to the oxidation being rate limited by deprotonation of the semiquinone. This is important physiologically because it effectively prevents futile cycling of the protein between its semiquinone and quinone states, which would waste valuable reducing equivalent in reducing Fld. The kinetics of this rate-limiting deprotonation event are pH sensitive, due to the pH dependence of the free energy of the $FldH^{\bullet}/Fld^{-}$ deprotonation step, indicating that flavodoxin will function most effectively as a low potential redox shuttle at acidic pH's, providing the potential to achieve regulation of flavodoxin function. In this regard, we note that sulfate metabolizing microorganisms, like *Desulfovibrio vulgaris*, possess an uptake mechanism in which sulfate ions are symported with protons, lowering the pH of the cytoplasmic compartment.[9,48] Furthermore, we note that this conclusion is in agreement with a previous study employing Fld as a low potential redox shuttle between ferredoxin−$NADP^{+}$ reductase and cytochrome *c*, where the reduction activity was observed to be 5-fold higher at pH 5.2 as compared to that at pH 8.2.[23]

Acknowledgment. We gratefully acknowledge the BBSRC and EPSRC for financial support, and Alex Green, Emilio Palomares, Franscine Duriaux, and Michael Grätzel for preparation of the SnO_2 electrodes.

JA0496470

(47) Vervoort, J.; Muller, F.; Mayhew, S. G.; van den Berg, W. A. M.; Moonen, C. T. W.; Bacher, A. *Biochemistry* **1986**, *25*, 6789−99.

(48) Cypionka, H. *Methods Enzymol.* **1994**, *243*, 3−14.